Annual Journal of Hydraulic Engineering, JSCE, Vol.53, 2009, February

CHARACTERISTICS OF LOCAL FLOW AND BED DEFORMATION AT IMPERMEABLE AND PERMEABLE SPUR DYKES

Hao ZHANG[1] and Hajime NAKAGAWA[2]

[1]Member of JSCE, Dr. of Eng., Assistant Professor, Disaster Prevention Research Institute, Kyoto University
(Shimomisu,Yoko-oji, Fushimi-ku, Kyoto 612-8234, Japan)
[2]Member of JSCE, Dr. of Eng., Professor, Disaster Prevention Research Institute, Kyoto University
(Shimomisu,Yoko-oji, Fushimi-ku, Kyoto 612-8234, Japan)

This paper presents the local flow patterns and bed deformation characteristics at a spur dyke with both laboratory experiments and numerical simulations. The spur dyke is of either an impermeable type or a permeable one with 50% permeability. The experiments are conducted in a straight tilting flume under non-submerged flow condition and clear-water scour regime. The flow velocities and bed topographies are measured with advanced experimental facilities and techniques such as electro-magnetic velocimetries, PIV (particle image velocimetry) and high-resolution laser displacement meter. A 3D morphological model is developed to simulate the complex local flow field and bed deformation process. The model is formulated using FVM (finite volume method) on a collocated unstructured mesh. Based on the study results, local flow patterns and morphological changes of the bed at different types of spur dykes are characterized. This is of great reference for the design and assessment of spur dykes.

Key Words : *Local flow, bed deformation, clear-water scour, impermeable spur dyke, permeable spur dyke*

1. INTRODUCTION

Spur dykes are typical man-made hydraulic structures and are widely constructed in alluvial rivers all over the world. Spur dykes are generally built perpendicular or at an angle to the channel bank or revetment, protruding into the watercourse. Historically, spur dykes were constructed to prevent channel banks or levees from erosion by diverting away approaching flows, to improve river navigation conditions by deepening main channel beds or to secure water supply and agricultural irrigation by maintaining suitable flow discharge and water level [e.g. 1), 2)]. Nevertheless, aesthetic and environmental impacts of spur dykes have attracted more and more attention since several decades before. Nowadays, spur dykes are also considered as a promising measure to enhance diversity of channel morphologies and riverine eco-systems [e.g. 1), 2), 3)].

An understanding of the turbulent flow and bed deformation in the vicinity of a spur dyke is a prerequisite to the design and construction of this kind of structure. Unfortunately, failures of spur dykes frequently occur in the world. Even recently, the authors' research group has witnessed such kind of failure sites several times. For example, the Betil and Enayetpur spurs on the Brahmaputra-Jamuna River for embankment protection in the Sirajganj District of Bangladesh experienced damages and rehabilitations many times after their completion in 2002. The authors visited the spur dykes in March 2008 and found that they were again under repair. In Japan, spur dykes for river restoration purpose on the Kizu River in Kyoto Prefecture were washed away in a flash flood soon after their completion in 2004. The spur dykes were re-designed and re-built, but the sustainability of the project is yet unknown. These examples demonstrate that scientific research and knowledge up to date are still far from enough. The Betil/Enayetpur spur dykes are impermeable, while both impermeable and permeable spur dykes were adopted in the Kizu River restoration project. According to previous researches with a series of impermeable and permeable spur dykes, the authors recommended the combination of the two kinds of spur dykes for practical use in order to achieve the maximum beneficial effect to the riverine ecosystem and still afford an effective control of the river flow[2]. However, the impacts of the two kinds of spur dykes on the local flow and bed deformation still necessitate characterization and quantification.

Scour depth and geometry at impermeable spur dykes have been the majority of existing researches. Since the scour process is closely related to the local flow, investigation including flow structure is also important and receives more and more attention with both experimental and numerical methods [e.g.3),4),5)]. Compared with an impermeable spur dyke, a permeable one is more environment-friendly but there are still very few studies [2]. A detailed review on related literatures and progresses has been made by the authors[6]. Here, fundamental experiments were conducted to investigate the flow pattern and bed deformation at an impermeable spur dyke and a permeable one. Detailed experimental data was obtained on bed geometries and flow velocities. 3D numerical simulations were carried out with a morphological model [7]. Based on experimental and numerical results, common points and different features of hydraulic and morphological impacts due to different spur dykes are discussed.

2. LABORATORY EXPERIMENTS

(1) Experiment setup

Experiments are conducted in a glass-sided tilting flume at the Ujigawa Open Laboratory, Kyoto University. The flume is 8m-long, 40cm-wide and 40cm-deep, with a 1.5m-long inlet tank at upstream (Fig.1). The slope of the flume was adjusted to 1/1000 in the experiments. A working area locates 4m downstream from the inlet tank. It is 1.7m long and is covered with 20cm-thick model sediment. The sediment consists of artificial materials made from sewage sludge ashes. The sediment is almost uniform, having a mean size of d=0.145cm and a specific gravity of s=1.9. The upstream and downstream parts of the working area are fixed with 20cm-thick wooden boards. A 50cm-long sediment trap is set at the end of the flume, followed by a tailgate. A spur dyke is attached to the flume, 1cm-thick and perpendicular to the flume side with a protruding length of 10cm. Two kinds of spur dykes have been tested: impermeable or permeable. The impermeable spur dyke is made of a painted wooden plate, not allowing water passing through it. The permeable one consists of a row of five cuboidal brass piles, having a permeability of 50%.

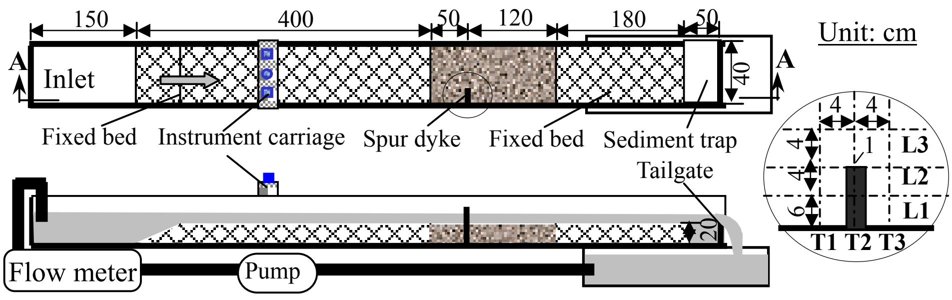

Fig.1 Experiment setup (Plan-view: Top; Section A-A: Bottom; Zoom-in: Right)

Table 1 Experiment conditions.

Discharge	0.0057 m^3/s	Sediment size	0.145 cm
Channel slope	1/1000	Sediment density	1.9 g/cm^3
Channel width	0.4m	Flow velocity	0.29 m/s
Flow depth	0.05m	u_*/u_{*c}	0.95
Spur length	0.1m	Re. number	14,250
Spur thickness	0.01m	Fr. number	0.41

(2) Experiment measurements

The spur dyke is non-submerged and the scour hole develops under clear-water scour regime. Experiment conditions are summarized in Table 1. Local scour developed rapidly in the first several minutes and showed insignificant changes after 1hr. Experiments continued for 2hr for each case. At the end of each experiment, a point gauge was utilized to measure the water level at some cross-sections. PVC tracers were distributed in the flume and videos were taken for PIV analysis. Then the pump was stopped. After the flume was completely drained out, a high-resolution laser displacement meter (Model LK-500, Keyence Co., Ltd.) was used to measure the bed deformation. After that, the scoured bed was moulded with instant cement. When the scoured bed was dried, water was pumped into the flume with the same discharge. The three velocity components at typical cross-sections were collected using electromagnetic velocimetries (Model ACM250-A, Alec Electronics, Co., Ltd). The locations of the measuring cross-sections were shown in Fig.1. At each measuring point, 300 samples were taken at a frequency of 10Hz.

3. NUMERICAL SIMULATIONS

(1) Numerical model

A numerical model is more cost-effective if well established and verified. The authors have developed a practicable morphological model [7]. In this model, the flow field is solved from the RANS (Reynolds-averaged

Navier-Stokes) equations with the k-ε turbulence closure. The wall-function approach is used near the walls and water surface is assumed unchangeable. Sediment transport direction follows the resultant direction of the near-bed flow and local bed slope. The transport rate is based on Ashida-Michiue's empirical formula and varies according to near-bed shear stress and local bed slope. Bed deformation is due to the sediment continuity equation in the bedload layer. The model formulation is based on an unstructured mesh, which provides great flexibility in resolving complex geometries and boundaries.

(2) Computational conditions

Computations are conducted under 4 kinds of conditions, varying in terms of spur dyke type and bed condition as shown in Table 2. In Case1 and Case2, the 2hr bed deformation process is simulated from an initial flat bed for impermeable spur dyke and permeable one, respectively. Case3 and Case4 are fixed bed simulations for the flow field based on the scoured bed topography.

Table 2 Computational conditions.

Case	Spur dyke	Bed condition	Time
1	Impermeable	Movable	2hr
2	Permeable	Movable	2hr
3	Impermeable	Fixed scoured	2hr
4	Permeable	Fixed scoured	2hr

Hybrid mesh consisting of hexahedra and prisms is used in the simulations. During the mesh generation, a mesh consisting of triangles and quadrilaterals is firstly generated in 2D plane. Then the 2D mesh is extended in the vertical direction according to corresponding measured water level and bed geometry. A plane view of the mesh system at different spur dykes is shown below.

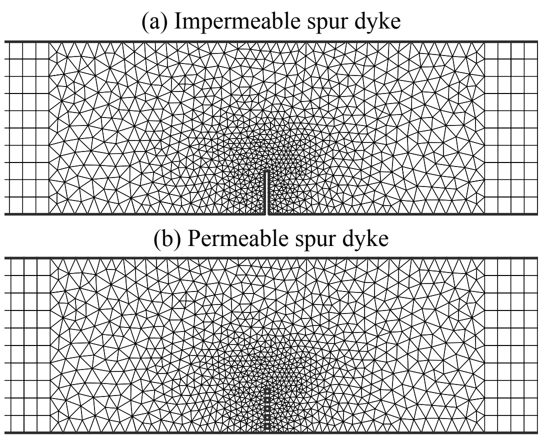

Fig.2 Plan-view of the mesh system around spur dyke.

4. RESULTS AND DISCUSSIONS

(1) Surface velocity at spur dyke

The mean velocity on the water surface under the scoured bed condition is shown in Fig.3. For ease of comparison, interpolation has been made.

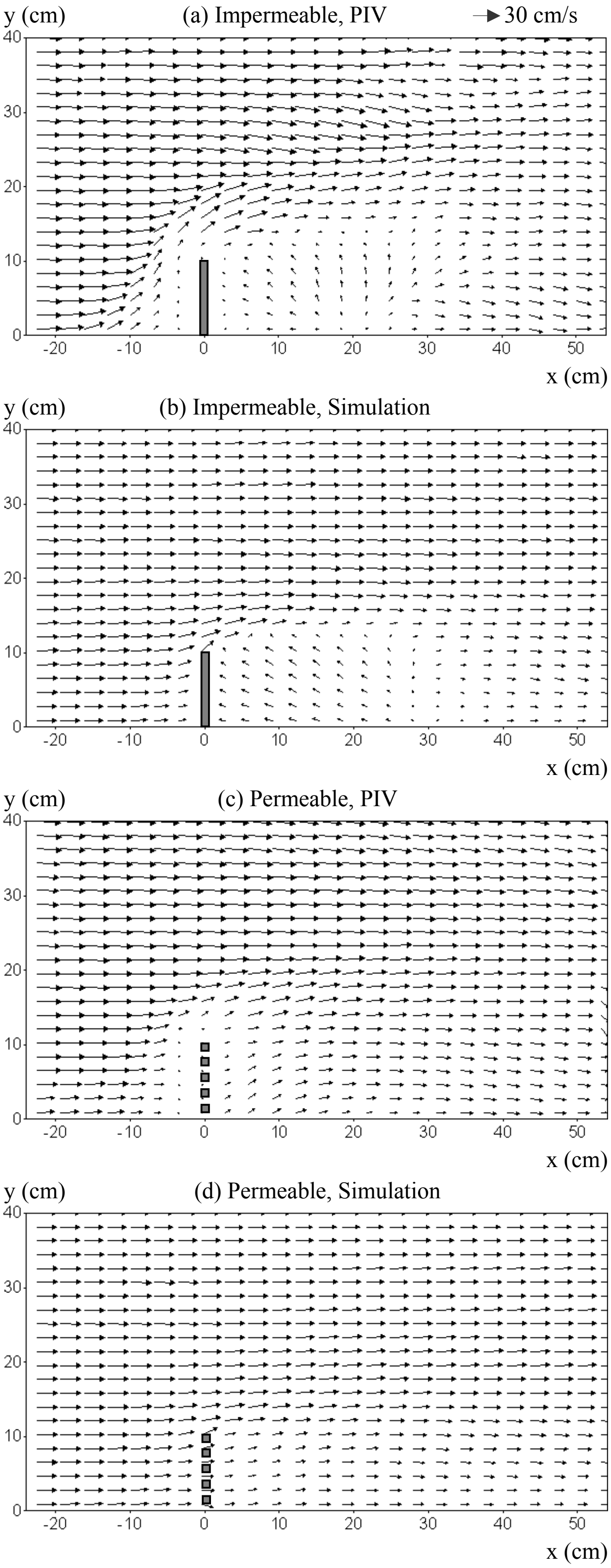

Fig.3 Velocity (u, v) on the free surface.

Taking a look at the PIV results, one may find some common points of the flow field between the impermeable spur dyke and the permeable one. In both cases, the flow velocities are obviously reduced when the flow approaches and passes the spur dyke. While in the main channel area, the flow velocities are significantly intensified. The wake flow area behind the spur dyke deserves special attention. In the impermeable case, the flow shows a fan-shaped structure. It spreads out from a point between x= 20cm-30cm, which is almost the intersection point of the flume side and the edge of the scour hole. This flow meets the separated flow from the spur dyke head and loses its identity in the mixing zone. The fan-shaped flow is a component of a vortex system as will be discussed later. On the other hand, the flow behind the permeable spur dyke does not show significant change in its direction. The differences stem from the local scour geometries and the spur dyke structures themselves. The local flow is complex and highly three-dimensional in impermeable case but is simple and longitudinally dominated in permeable case. Comparing the simulation results with the PIV results, one may find that there are good agreements in most of the flow physics. In the proximity of the spur dyke, it should be mentioned that the amount of PIV data is very little. The flow structure is not well resolved. But in the numerical simulations, the flow structure is very clear. When the flow approaches the spur dyke, it is diverted to the head of the spur dyke in impermeable case but most of the flow passes the spur dyke and a small part is diverted to the head in permeable case. Consequently, the angles of flow separation are quite different in two cases.

Since the flow in impermeable case is obviously 3D, an investigation on the detailed flow structure is necessary and important to understand the scour process. The velocity profiles at typical transverse and longitudinal sections are hence discussed.

(2) Transverse flow velocity

Velocity vectors (v, w) at three typical transverse cross-sections (T1, T2 and T3) of the impermeable case are shown in Fig.4. The locations of these sections have been sketched in Fig.1. Sections T1 and T3 locate 4cm upstream and downstream from the centerline of the spur dyke, respectively. Section-T2 passes the centerline of the spur dyke.

Along all these sections, a component of the horse-shoe vortex is evidently observed in the scour hole around the head of the spur dyke. Sediment absorbed by the horse-shoe vortex will be directed away from the spur dyke. With the transport of the vortex system downstream, the center of the vortex becomes farther away from the spur dyke. The vortex center locates at y=17cm at the upstream section (T1) but changes to y=20cm at the downstream section (T3). The locations of the horse-shoe vortex in the simulation are slightly different from those in the experiment laterally. An over-estimation of the flow separation angle at the head of the spur dyke is the probable reason. It is very evident, for example, that the flow along Section-T3 is almost vertical from y=12cm to y=16cm in the experiment plot but owns a small transverse velocity component in the simulation. It is also noticed that the horse-shoe vortex is confined in the scour hole beneath the original bed in both experiment and simulation, which coincides with the results in previous researches [e.g.4), 8)]. Moreover, there are two rotating cells along Section-T3. Besides the horse-shoe vortex at the head of the spur dyke, there is another vortex system in the wake zone area. This vortex is in an opposite direction compared with the horse-shoe vortex. On the surface, it has a fan-shaped flow structure as observed in Fig.3a and Fig.3b. This vortex is independent from the horse-shoe vortex and occupies most of the water column. Due to the presence of this vortex, sediment is directed towards the side of the flume. This deepens the scour hole in the wake area and results in sediment deposition along the flume side.

(3) Longitudinal flow velocity

Velocity vectors (u, w) at three typical longitudinal sections (L1, L2 and L3) of impermeable case are shown in Fig.5. These cross-sections locate at a distance of 6cm, 10cm and 14cm from the flume side (Fig.1), respectively. In all these plots, a reasonably good matching between the experimental and numerical results is observed.

A downflow and the horse-shoe vortex occur in front of the spur dyke due to the pressure gradient there as shown in Section-L1 and Section-L2. Since the spur dyke is not present in Section-L3, the horse-shoe vortex due to the flow separation extends to the downstream of the spur dyke and soon becomes a part of the general turbulence. In all these sections, the horse-shoe vortex is confined in the scour hole area. Taking into account the pictures of the horse-shoe vortex in other projection planes as described in previous contexts, one may conclude that the horse-shoe vortex is closely related to the scour geometry and plays a crucial role in the local scour development.

Behind the spur dyke, a circulation cell is observed in the wake zone just below the water surface in Section-L1 and Section-L2. The circulation is in an anti-clockwise direction. Referring the information on the surface (Fig.3) and Section-T3 in Fig.4, it is clear that this vortex has a close relation with the scour geometry behind the spur dyke and is another important scour engine.

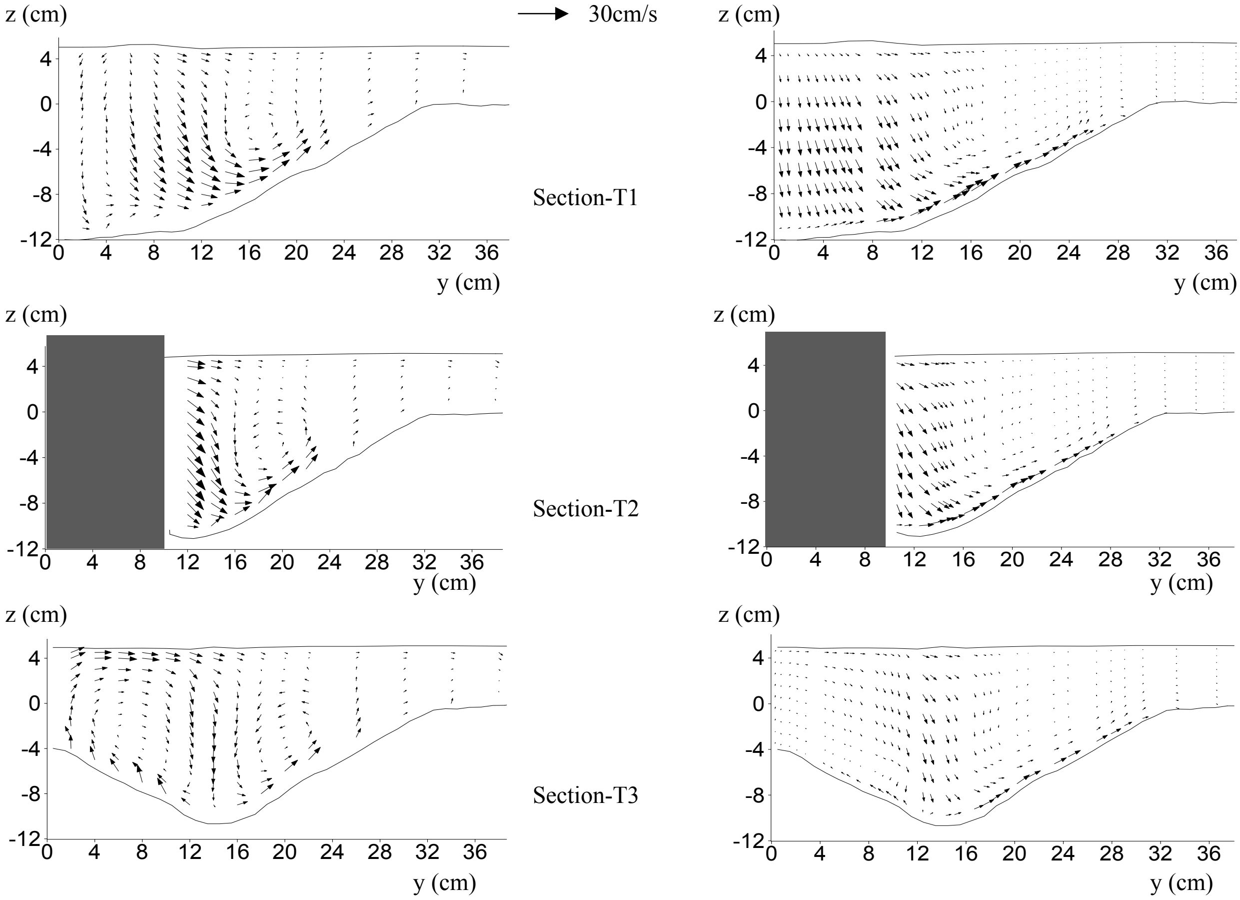

Fig.4 Velocity (v, w) at typical transverse sections in impermeable case (Experiment: Left; Simulation: Right).

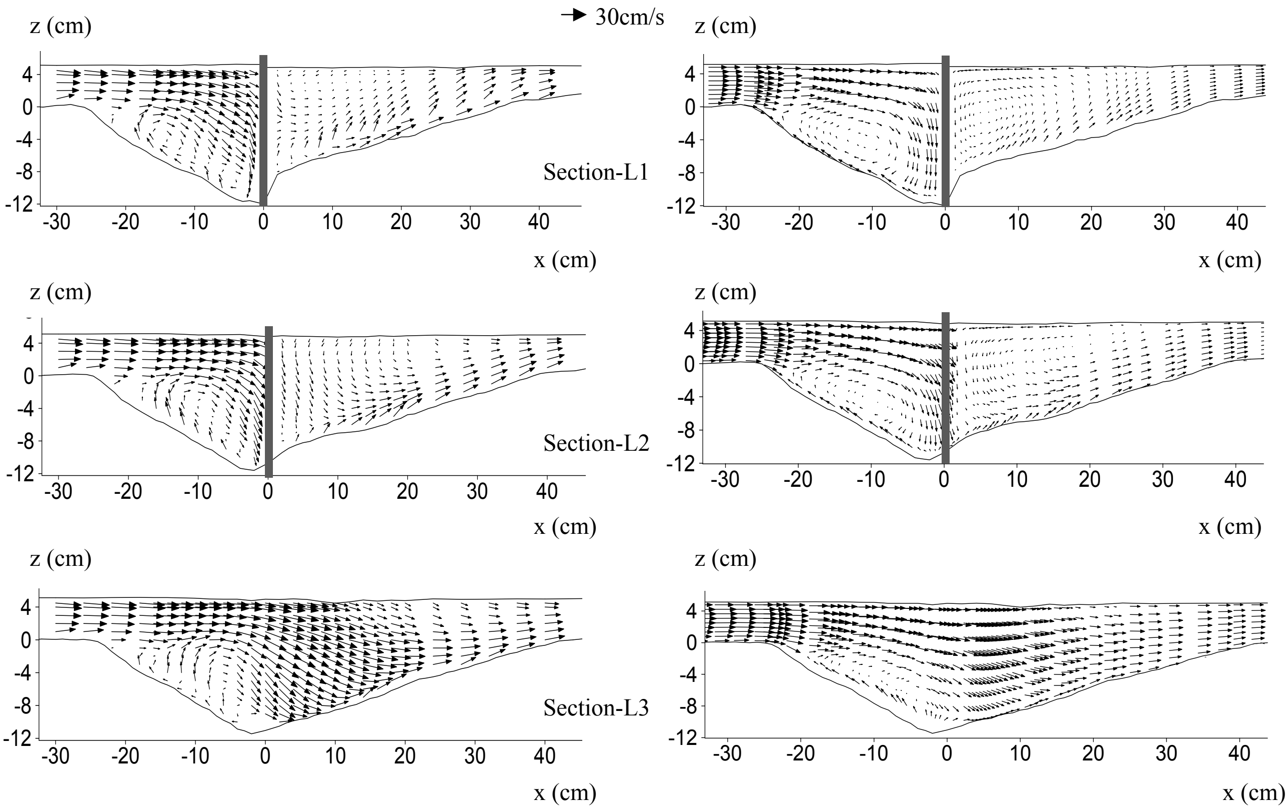

Fig.5 Velocity (u, w) at typical longitudinal sections in impermeable case (Experiment: Left; Simulation: Right).

(4) Bed deformation

The final bed contour is shown in Fig.6 and Fig.7.

The simulated scour holes are smaller than those in the experiment. The under-estimation of the velocity magnitude and the insufficiency in linking near-bed flow field and sediment movement are the probable reasons. Nevertheless, fundamental characteristics of the bed deformation are reasonably reproduced.

The maximum scour depth and scour area in the impermeable case are much larger than those in the permeable one. The difference is caused by different flow structure and scour mechanism. In permeable case, scour is due to flow separation at the spur dyke head and compressed vortex system in-between two consecutive piles. While in the impermeable case, scour initiates from flow separation at the spur dyke head. With the development of local scour hole, a horse-shoe vortex and a wake vortex become major engines. Behind the spur dyke, deposition appears in either case due to reduction of flow velocity there.

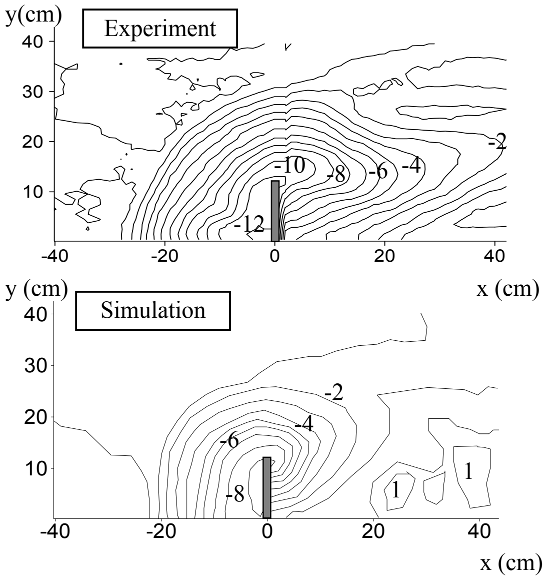

Fig.6 Bed deformation at impermeable spur dyke

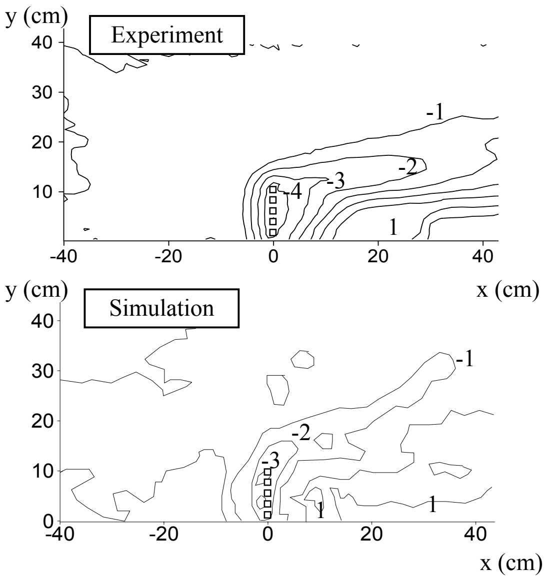

Fig.7 Bed deformation at permeable spur dyke

5. CONCLUSIONS

Impermeable spur dyke has great impacts on flow structure. The flow velocity is affected in both direction and magnitude, resulting in significant scour around the spur dyke head. The scour then gradually expands outwards. With the development of scour, the 3D characteristics of the flow become more and more evident. The flow is generally characterized by complex vortex systems. The permeable spur dyke reduces the velocity of the flow passing through it. Nevertheless, the direction of the flow velocity is not changed much. Scour occurs at both the head and the body of it. There are some common points concerning the hydraulic and morphological consequences of impermeable and permeable spur dykes. Flow separation takes place around the head of either impermeable spur dyke or permeable one, although the separation angle is much larger in the former case. The flow separation results in similar bed deformation at the heads of both spur dykes. Wake flow zone exists in both cases and sediment deposition is observed in the downstream of either spur dyke. Desirable flow and channel morphology is achievable if the two types of spur dykes are effectively combined. A numerical model is powerful for the design and assessment of spur dykes but still awaits further refinement.

REFERENCES

1) Yamamoto, K.: *Japan's Spur Dykes*, Sankaido Publishing Co., LTD, 1996 (in Japanese)
2) Zhang, H., Nakagawa, H., Ishigaki, T., Muto, Y. and Khaleduzzaman, A.T.M.: Flow and bed deformation around a series of impermeable and permeable spur dykes, *MPMD2005*, pp. 197-202, Kyoto, Jan. 12-15, 2005
3) Nagata, N., Hosoda, T. Nakato, T. and Muramoto, Y.: Three-dimensional numerical model for flow and bed deformation around river hydraulic structures, *J. Hydraul. Eng., ASCE*, Vol. 131. No. 12, pp. 1074-1087, 2005
4) Michiue, M. and Hinokidani, O.: Calculation of 2-dimensional bed evolution around spur-dike, *Annual J. of Hydraul. Eng., JSCE*, vol.36, pp.925-930 (in Japanese)
5) Onda, S., Hosoda, T. Kimura, I. and Iwata, M.: Numerical simulation on local scouring around a spur dyke using equilibrium and non-equilibrium sediment transport models, *Annual J. Hydraul. Eng., JSCE*, Vol. 51, pp. 943-948, 2007. (in Japanese)
6) Zhang, H. and Nakagawa, H.: Scour around spur dyke: recent advances and future researches, *Annuals Disa. Pre. Res. Inst.*, Kyoto Univ., No.51B, 2008.
7) Zhang, H., Nakagawa, H., Muto, Y., Baba, Y. and Ishigaki, T.: Numerical simulation of flow and local scour around hydraulic structures, *Riverflow2006*, pp. 1683-1693, 2006
8) Barbhuiya, A.K. and Dey, S.: Vortex flow field in a scour hole around abutments, *Int. J. Sedi. Res.*, vol.18, No.4, pp. 310-325, 2003

(Received September 30, 2008)